Water Research 255 (2024) 121458

Contents lists available at ScienceDirect

Water Research

journal homepage: www.elsevier.com/locate/watres

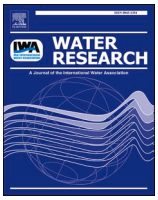

Experimental and density functional theory investigation of surface-modified biopolymer for improved adsorption of mixtures of per- and polyfluoroalkyl substances in water

Aswin Kumar Ilango [a,*], Parandaman Arathala [b], Rabi A. Musah [b], Yanna Liang [a]

[a] Department of Environmental and Sustainable Engineering, University at Albany, State University of New York, 1400 Washington Avenue, Albany, NY 12222, United States
[b] Department of Chemistry, University at Albany, State University of New York, 1400 Washington Avenue, Albany, NY 12222, United States

ARTICLE INFO

Keywords:
PFAS
Aerogel flakes
Adsorption
>99 % removal in tap water
Regeneration and reuse
DFT calculations

ABSTRACT

Glutaraldehyde (GTH) cross-linked chitosan (CTN) biopolymer-based and polyethyleneimine (PEI) functionalized (GTH—CTNPEI) aerogels were proven promising for removing mixtures of long- and short chain per- and polyfluoroalkyl substances (PFAS) in water. In this study, to further improve the performance of the aerogel for short-chain PFAS and undecafluoro-2-methyl-3-oxahexanoic acid (GenX) removal, GTH—CTNPEI aerogel chunks with an average size of 13.4 mm were turned into flakes with an average size of 9.1 mm. The GTH—CTNPEI flakes achieved >99 % removal of all target PFAS, including long- and short-chain PFAS and >97 % for GenX after 10 h. In addition, the flakes can be regenerated and reused for at least four cycles. When added to tap water spiked with PFAS at initial concentrations of 30, 70, or 100 ng/L, the flakes removed almost 100 % of all tested PFAS. Mechanistic investigations using density functional theory (DFT) revealed strong stabilizing hydrophobic and electrostatic interactions between the aerogels and PFAS, with GTH—CTNPEI to PFAS binding energies ranging between -24.0 – -30.1 kcal/mol for PFOA; -41.3 – -48.5 kcal/mol for PFOS; and -40.5 – -47.3 kcal/mol for PFBS. These results demonstrate the great potential of the flakes for removing PFAS from drinking water, surface water, and groundwater.

1. Introduction

Per- and polyfluoroalkyl substances (PFAS) are generally recognized as "forever chemicals" due to their persistence in the environment (Brunn et al., 2023; Glüge et al., 2021). Among more than 9000 PFAS, the legacy long-chain perfluoroalkyl acids (PFAAs), such as perfluorooctanoic acid (PFOA) and perfluorooctanesulfonic acid (PFOS) are the most widespread in the environment and even in human bodies (Cordner et al., 2021; Li et al., 2020, 2022b). In June 2022, the U.S. Environmental Protection Agency (EPA) issued interim lifetime health advisory limits for PFOA and PFOS in drinking water at very low concentrations of 0.004 and 0.02 ng/L, respectively (Rabinow, 2022). Due to their resistance to degradation, potential toxicity, and tendency to bioaccumulation, actions have been taken by industries/regulatory agencies in the US starting from 2000 to stop the production and use of PFOA and PFOS (Butenhoff et al., 2009; Sunderland et al., 2019).

Their replacements, such as short-chain perfluoroalkyl carboxylic acids (PFCAs) (C_4—C_6), short chain perfluoroalkylsulfonic acids (PFSAs) (C_4), long-chain PFCA (C_7), long-chain PFSA (C_6) (Buck et al., 2011), undecafluoro-2-methyl-3-oxahexanoic acid (GenX), and 6:2 fluorotelomer sulfonic acid (6:2 FTS) have been used to replace PFOA, PFOS and other long chain PFAAs in various applications, such as modern aqueous film-forming foam (AFFF), food contact substances, chemical coatings and production of fluoropolymers (EPA, 2021). Most of these alternatives, although reported as less bioaccumulative compared to PFOA and PFOS, have been shown to be environmentally and biologically stable and may persist in the natural environment (Bao et al., 2018; Brendel et al., 2018; Smalling et al., 2023; Teymoorian et al., 2023; Wang et al., 2015). Therefore, removal of legacy as well as these other emerging PFAS is urgently needed to safeguard the water environment.

The conventional method of removing PFAS from water is through adsorption (Jiang et al., 2022; Jiang et al., 2021) using granular activated carbon (GAC) (Ilango et al., 2023b; McCleaf et al., 2017; Woodard et al., 2017). GAC, however, is known as a non-selective sorbent.

* Corresponding author.
E-mail address: ailango@albany.edu (A.K. Ilango).

https://doi.org/10.1016/j.watres.2024.121458
Received 1 December 2023; Received in revised form 27 February 2024; Accepted 11 March 2024
Available online 12 March 2024

Specific to PFAS removal, it has drawbacks of slow kinetics and inefficiency in removing short chain PFAS (Gibert et al., 2013; Saha et al., 2021). Additionally, considering the fact that GAC is produced mostly from coal through harsh thermal and/or chemical processes, it is not truly a sustainable material from both environmental and economic perspectives. To meet ever-increasing regulatory requirements, sustainable, green, and low-cost sorbent materials are needed (Ilango and Liang 2023; Li et al., 2022a; Militao et al., 2021).

One promising material is surface-modified biopolymers i.e., glutaraldehyde cross-linked chitosan biopolymer-based and polyethylenimine functionalized (GTH—CTNPEI) aerogel (Ilango et al., 2023a). This aerogel has been shown to successfully remove a mixture of 12 PFAS from water at 10 μg/L each, with >99.9 % removal of eight long and relatively hydrophobic PFAS. More importantly, this aerogel was predicted to possess a sorption capacity of 12,133 mg PFAS/g sorbent. However, its effectiveness is limited to 70–90 % for short-chain PFAS and GenX due to its limited porosity and large particle size. To improve the aerogel's efficacy toward removing all PFAS, further development of materials with higher porosity (Li et al., 2021) and smaller particle size is necessary (Ching et al., 2023).

This study was thus designed to further improve the performance of the aerogel in capturing a mixture of PFAS in water. First, the theoretical sorption capacity predicted by the isotherm models was confirmed through experimental studies. Second, the sorption performance of the aerogel with a smaller particle size than what was reported before was evaluated. Third, the regenerability and reusability of the aerogel were assessed. Fourth, the aerogel's use for removing PFAS in tap water in the ng/L range was studied. Finally, density functional theory (DFT) simulation was used to study the binding mechanisms between PFAS molecules and the GTH—CTNPEI aerogel at the molecular level. Results from this study help advance understanding of using GTH—CTNPEI aerogel for removing PFAS from contaminated water.

2. Materials and methods

2.1. Validation of sorption capacity of GTH—CTNPEI aerogel for PFAS removal

The procedure for synthesizing the GTH—CTNPEI aerogel was reported previously (Ilango et al., 2023a). Briefly, 0.1 g of CTN was dissolved in a solution of 2 % acetic acid (v/v) and GTH (5 wt.%). Then, a PEI solution [1 mL of PEI (50 % in water) + 4.90 mL of deionized water] was added to the mixture dropwise and stirred for 3 h until a uniform emulsion was obtained. After incubation and freeze-drying, the obtained GTH—CTNPEI aerogel was stored in a tightly sealed container at 25 °C for further use.

In our previous publication (Ilango et al., 2023a), the theoretical maximum sorption capacity of the aerogel was estimated to be 12,133 mg/g as determined using a Sips isotherm. To validate this extremely high sorption capacity, we used the same material to capture PFOA at initial concentrations of 300, 500, 800, or 1200 mg/L, with initial masses of 15, 25, 40 or 60 mg respectively in 50 mL deionized water. To measure PFOA at time 0 min, 500 μL of the PFOA solution was withdrawn from each tube before adding 5 mg of the aerogel. After adding the sorbent, all tubes were placed on a rotatory shaker at 120 rpm at room temperature. The subsamples collected at 2, 18, 24 and 48 h were centrifuged and filtered through 0.2 μm nylon filters before analysis by LC-MS-MS as detailed in SI Text S1.

2.2. GTH—CTNPEI aerogel flakes and PFAS sorption experiment

To generate GTH—CTNPEI flakes, chunks of GTH—CTNPEI aerogel (Ilango et al., 2023a) were cut into small pieces and ground using a mortar and pestle. The resulting flakes were stored in a tightly sealed container at 25 °C for further use.

Adsorption experiments were conducted in batch mode in triplicate. In short, to each polypropylene conical tube, a 50-mL PFAS solution comprised of 12 PFAS (PFCAs (C_6—C_{11}), PFSAs (C_4, C_6, and C_8), GenX, 6:2 FTS, and 2-*N*-ethyl perfluorooctane sulfonamidoacetic acid (N-EtFOSAA)), each at 10 μg/L or 500 ng was added. The physicochemical properties of the PFAS investigated in this study are shown in Table S1. Before adding 25 mg GTH—CTNPEI flakes to the solution to reach a dose of 500 mg/L, 500 μL of the PFAS solution was withdrawn from each tube. These samples were used for measurement of PFAS at time 0 min. Once the sorbent was added, all tubes were kept on a rotatory shaker at 120 rpm. Subsamples from each tube were collected at 4 and 10 h to analyze PFAS concentrations by LC-MS-MS as explained in Text S1.

2.3. Regeneration and reuse of the GTH—CTNPEI flakes

To understand whether the GTH—CTNPEI flakes can be regenerated and reused, PFAS recovery tests following the adsorption experiment were performed. The adsorption test was conducted with flakes at 500 mg/L (25 mg) in 50 mL of the same PFAS mixture mentioned above for 10 h. After that, the PFAS-laden GTH—CTNPEI flakes were collected by filtration and dried. The dried flakes were subject to extraction by 2 % methanolic ammonium hydroxide (6.6 mL of 30 % ammonium hydroxide in 93.4 mL methanol, according to the 4th Draft of EPA Method 1633). Following three rounds of extraction using the basified methanol on a rotary shaker, each round for 1 h, the flakes were washed with deionized water three times and dried at 65 °C overnight. The regenerated GTH—CTNPEI flakes were then used to remove the PFAS mixture to assess their reusability performance. This process was repeated for four cycles. All methanol extracts and water washes were processed for PFAS measurements by LC-MS-MS (Text S1).

2.4. Use of GTH—CTNPEI flakes for removing low concentrations of PFAS in tap water

For this purpose, GTH—CTNPEI flakes at 500 mg/L (25 mg) were added to PFAS-spiked tap water at University at Albany. A total of twelve PFAS were studied. Each PFAS was tested at an initial concentration of 30, 70, or 100 ng/L (1.5, 3.5 or 5 ng each). Triplicate subsamples withdrawn at 1, 4, 10, 24 and 48 h were processed for analysis of PFAS by LC-MS-MS. Based on the total mass of each PFAS added to 50 mL aqueous solutions, the mass of PFAS removed through sorption or recovered by methanol washing was calculated using eqns. (S1) to (S4) while the sorption capacity of the aerogel was calculated using eqn. (S5) as given in SI Text S2.

2.5. Computational methodology

We used density functional theory (DFT) modeling to understand better the molecular level interactions between the GTH—CTNPEI aerogel and PFAS. The geometries of CTN, PEI, aerogel, PFAS (PFBS, PFOA, and PFOS) (Fig. 1), and various possible aerogel-PFAS complexes were optimized using the M06–2X hybrid density functional along with the 6–31+*G*(d,p) basis set (Peverati and Truhlar, 2014; Zhao and Truhlar, 2008). This level of theory is well suited for computing non-covalent interactions, because of its ability to describe medium-range electron correlations of charged anionic and cationic species, and for the characterization of van der Waals interactions in dimer complexes (Giroday et al., 2014; Rayne and Forest, 2010; Zhao and Truhlar, 2006).

Various studies have reported the use of M06–2X level calculations to determine the structures, hydrogen bonding, and binding energies of various complexes containing C, H, S, N and O-atom containing compounds (Arathala and Musah, 2020, 2022). Diffuse functions were added to the basis set for the non-hydrogen atoms in order to capture the electronic effects in charged anionic and cationic species. Further, all geometry optimization in aqueous solutions and harmonic vibrational frequency calculations were carried out using the solvation model density (SMD) variation of the polarizable continuum solvation model

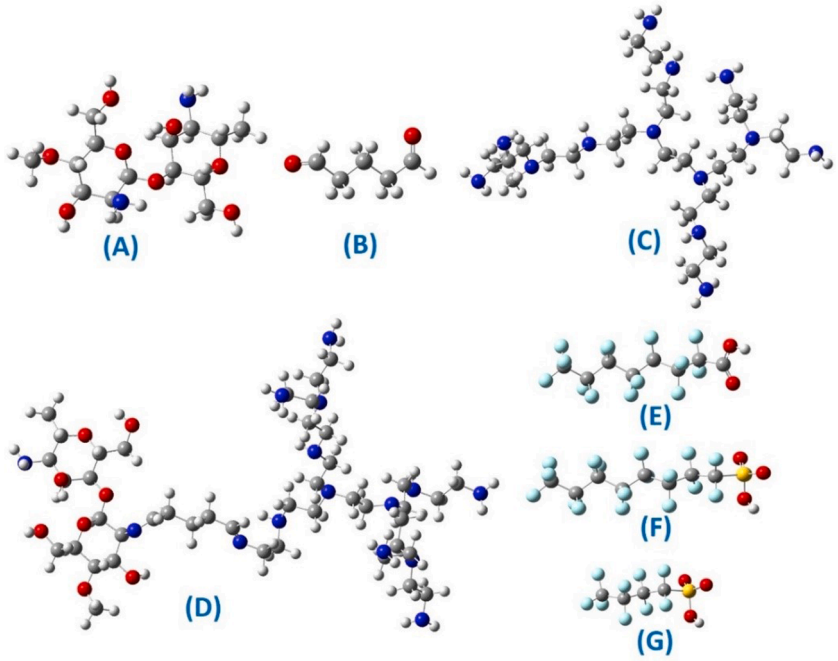

Fig. 1. Molecular geometries of: (A) chitosan, (B) glutaraldehyde, (C) polyethylenimine, (D) GTH—CTNPEI aerogel, (E) PFOA, (F) PFOS, and (G) PFBS. The black, white, blue, yellow, cyan-blue, and red colors represent C, H, N, S, F and O-atoms, respectively.

(Marenich et al., 2009). The dielectric constant of water ($\varepsilon = 78.3553$) was used to mimic the solvation environment between the aerogel and three different PFAS molecules, similar to the experimental study. All optimized stationary structures were confirmed to be minima by harmonic vibrational frequency calculations, and there were no imaginary frequencies. All analyses were performed with the Gaussian 16 suite of programs (Frisch et al., 2016). The aerogel-PFAS complexes were formed at three binding locations, as explained in Section 3.5.

The binding energies (ΔE_{bind}) of all the possible aerogel-PFAS complexes were calculated as the energy difference between the respective optimized aerogel-PFAS dimer complex and the energy of optimized monomers (aerogel and PFAS (PFOA or PFOS or PFBS)) as given in Eq. (1),

$$\Delta E_{bind} = E_{dimer} - (E_{R_1} + E_{R_2}) \quad (1)$$

where, E_{dimer} represents the total energy of an aerogel-PFAS dimer complex, and E_{R_1} and E_{R_2} represent the total energies of their respective aerogel and PFAS monomers. In addition, we also estimated the Gibbs free energy (ΔG) for all studied aerogel-PFAS complexes using Eq. (2),

$$\Delta G = G_{dimer} - (G_{R_1} + G_{R_2}) \quad (2)$$

where, G_{dimer} is the Gibbs free energy of an aerogel-PFAS dimer complex, and G_{R_1} and G_{R_2} represent the total Gibbs free energies of the aerogel and PFAS (PFBS or PFOA or PFOS) monomers. The ΔE_{bind} and ΔG for all aerogel-PFAS dimer complexes were calculated relative to the values for their corresponding separated monomers at the M06–2X/6–31+G(d,p) level. The Cartesian coordinates for aerogel, PFAS (PFOA, PFOS, and PFBS), and the various possible aerogel-PFAS complexes are provided in Table S2. In addition, the computed total electronic energies along with the zero-point energy (ZPE) corrected electronic energies of the respective species computed at the M06–2X/6–31+G(d,p) level are provided in Table S2.

3. Results and discussion

3.1. Sorption capacity validation of GTH—CTNPEI aerogel chunks

As mentioned above, according to the Sips sorption isotherm, the GTH—CTNPEI aerogel had a maximum adsorption capacity of 12,133 mg PFAS/g at 24 h (Ilango et al., 2023a). Compared to most PFAS sorbents with a sorption capacity of hundreds of mg/g (Karoyo and Wilson 2013; Liu et al., 2022), this capacity is exceptionally high. To confirm such a high capacity, PFOA was used as a representative PFAS. As shown in Fig. S1, the experimental sorption capacity increased with time from 0 to 24 h and increased with increasing initial PFOA concentration. When added to a solution of PFOA at 1.2 g/L, the GTH—CTNPEI aerogel sorbed 5929 mg PFOA/g, which is around six times its own weight. Based on the trend of increasing sorption capacity with increasing PFOA concentration, it is reasonable to expect higher capacity when the initial PFOA concentration is higher than 1.2 g/L. Higher concentrations were not tested in this study since they are rarely observed in the environment. Nevertheless, the GTH—CTNPEI aerogel was proven to have unusually high PFAS sorption capacity.

3.2. Sorption performance of GTH—CTNPEI aerogel flakes for removing PFAS in ultrapure water

Theoretically speaking, lowering the particle size of a sorbent tends to increase its sorption capacity due to increased surface area (Vu and Wu, 2020, 2022; Wu et al., 2020). To further increase sorption capacity, aerogel pieces or chunks of an average size of 13.4 mm were ground into flakes with an average size of 9.1 mm. As shown in Fig. S2, the GTH—CTNPEI flakes achieved >98 % removal of all short-chain PFAAs, including PFBS, PFHxA, and PFHpA, as well as all long and relatively hydrophobic PFAS at 10 μg/L (500 ng) each after 10 h. For GenX, the removal efficiency was >97 % at hour 10. Compared to aerogel chunks which removed 70–90 % of GenX and a few short-chain PFAAs after 24 h (Ilango et al., 2023a), the flakes apparently exhibited higher capacity and a faster rate of sorption of all target PFAS.

3.3. Reusability assessment of GTH—CTNPEI flakes

To test whether the flakes can be reused after the PFAS adsorption process, the PFAS-laden GTH—CTNPEI flakes were thrice washed with both 2 % methanolic ammonium hydroxide and deionized water, in tandem. As indicated in Table S3, the basic methanol wash recovered at least >90 % of all 12 PFAS in the spent sorbent. Once the washed sorbent was rinsed with water, it was used for sorption and desorption again (referred to as cycle #2). Similarly, the sorbent was reused twice more (two cycles) and >99 % recovery of all PFAS was achieved for every cycle. The full recovery of PFAS in the spent sorbent could be due to a reversal of the sorption where electrostatic and hydrophobic interactions play significant roles.

The regenerated GTH—CTNPEI flakes showed outstanding adsorption capability. As seen in Fig. 2, the removal efficiency of all tested PFAS did not significantly decrease with repeated uses, at least for the four cycles tested in this study. As shown in Table S3, the total mass of PFAS added varied between 3501.9 ± 233.4 and 5290.0 ± 309.0 ng, while the total mass of PFAS removed by sorption was from 3406.1 ± 288.1 to 5119.6 ± 133.4 ng in the sorption cycles 1 to 4. Based on this, the sorption capacity of the aerogel flakes for total PFAS varied between 136.2 ± 9.8 and 204.8 ± 6.0 ng/mg. The fact that these capacities are much lower than the theoretical value of 12,133 μg PFAS/mg hinted that the aerogel flakes were far from being saturated by the tested PFAS, and that the 25 mg flakes had the capacity to remove PFAS in large volumes of water contaminated by the same set of PFAS. Additionally, the revelation that the GTH—CTNPEI flakes were able to retain their sorption capacity (ng/mg) (Table S3) after repeated regeneration and reuse demonstrated that the molecular structure of the sorbent was not disrupted by methanol washing. The wash simply removed sorbed PFAS. Once the PFAS was removed, the sorbent was able to again capture solubilized PFAS.

Similar findings have been reported for other bio-based sorbents. In a study by Ateia et al. (2018), it was found that methanol can recover 100 % of PFOA from PEI functionalized carboxymethylcellulose (PEI-f-CMC). This sorbent can be reused for up to eight cycles for PFOA removal at 1 mg/L and pH 6.5. Similarly, PEI and quaternary amine functionalized pine bark (PG-PB) could be reused for PFOA sorption for up to three cycles (Ren et al., 2023). In the first and second desorption cycles, more than 70 % and 85 % of PFOA was recovered, respectively by methanol through disruption of hydrophobic interactions (Zaggia et al., 2016). Disrupting the electrostatic interactions between PFOA and the quaternary nitrogen group by NaOH was reported to be less effective compared to methanol. Decreased removal efficiency of PFOA was observed in the third cycle.

Other promising PFAS sorbents, such as surface modified clays (Dong et al., 2021), cannot be regenerated using methanol and other organic solvents because of the destruction they cause to the clay's chemical structure. Regarding GAC (Márquez et al., 2022), high temperatures are needed for thermal regeneration. This thermal regeneration, however leads to a 5–15 % of loss of carbon by friction (Watanabe et al., 2018), and decreases the micropore volume of virgin GAC from 0.151 to 0.027 cm^3/g after the third regeneration cycle as reported by Son et al. (2020).

3.4. Use of GTH—CTNPEI flakes for removing PFAS from tap water

To investigate whether the GTH—CTNPEI flakes were able to remove PFAS in finished drinking water, we tested their removal performance toward PFAS at 30, 70, and 100 ng/L in tap water. As demonstrated by Fig. 3, all long-chain PFAS were removed entirely in 1 h. The short-chain PFAS, such as PFBS, PFHxA, PFHpA, and GenX, needed a longer time for maximum removal. But after 24 h, the removal efficiencies for these tough-to-remove PFAS were all above 95 % except GenX at an initial concentration of 100 ng/L, even at 48 h. Since GenX does not appear as ubiquitously as other PFAS in drinking water matrices, its lower removal efficiency should not cause much concern. As shown in Table S4, the total mass of PFAS added to the 50 mL of tap water varied between 9.33 ± 1.75 and 39.24 ± 1.96 ng, while the total mass of PFAS removed was from 9.33±1.75 to 38.91±2.08 ng at 48 h. Based on these results, the sorption capacity of the aerogel flakes was calculated as 0.37±0.07 to 1.55±0.083 ng/mg. The lower removal of both PFOA and GenX in tap water when compared to that of ultrapure water (Fig. S2) could signal

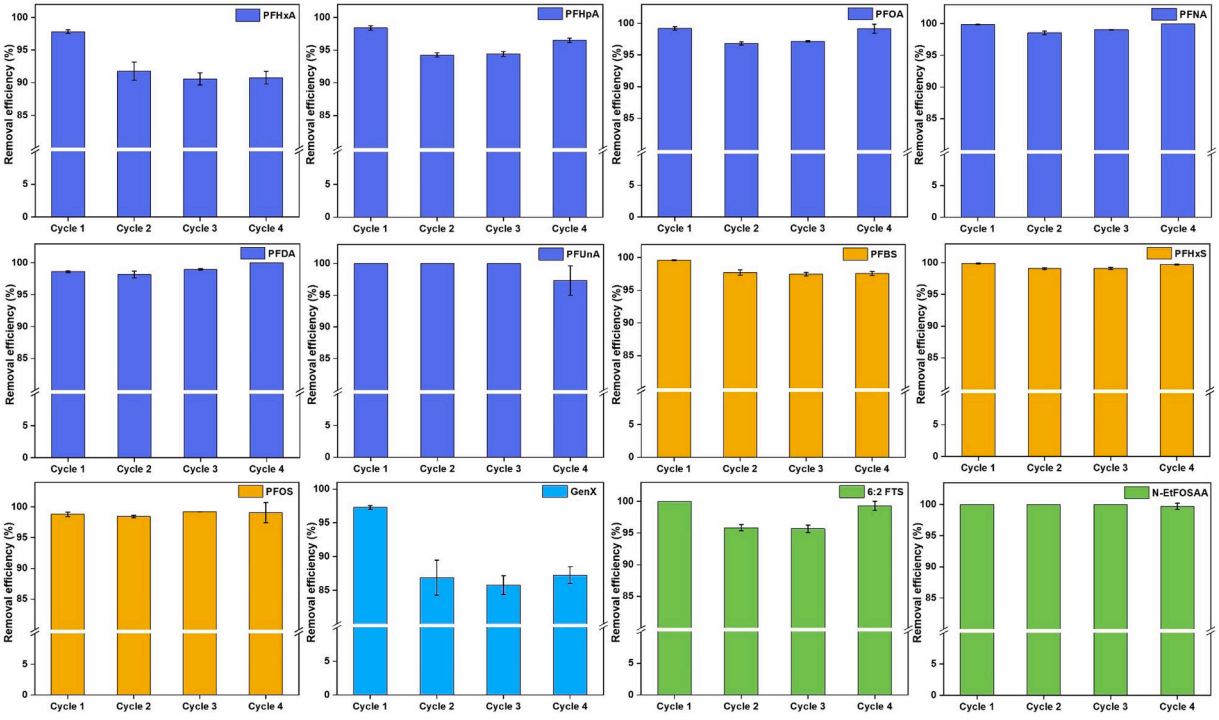

Fig. 2. Removal efficiency of PFAS mixtures after four cycles of regeneration and reuse. Initial PFAS concentration: 10 μg/L, and aerogel flakes dose: 500 mg/L. Error bars represent the standard deviations of triplicate measurements.

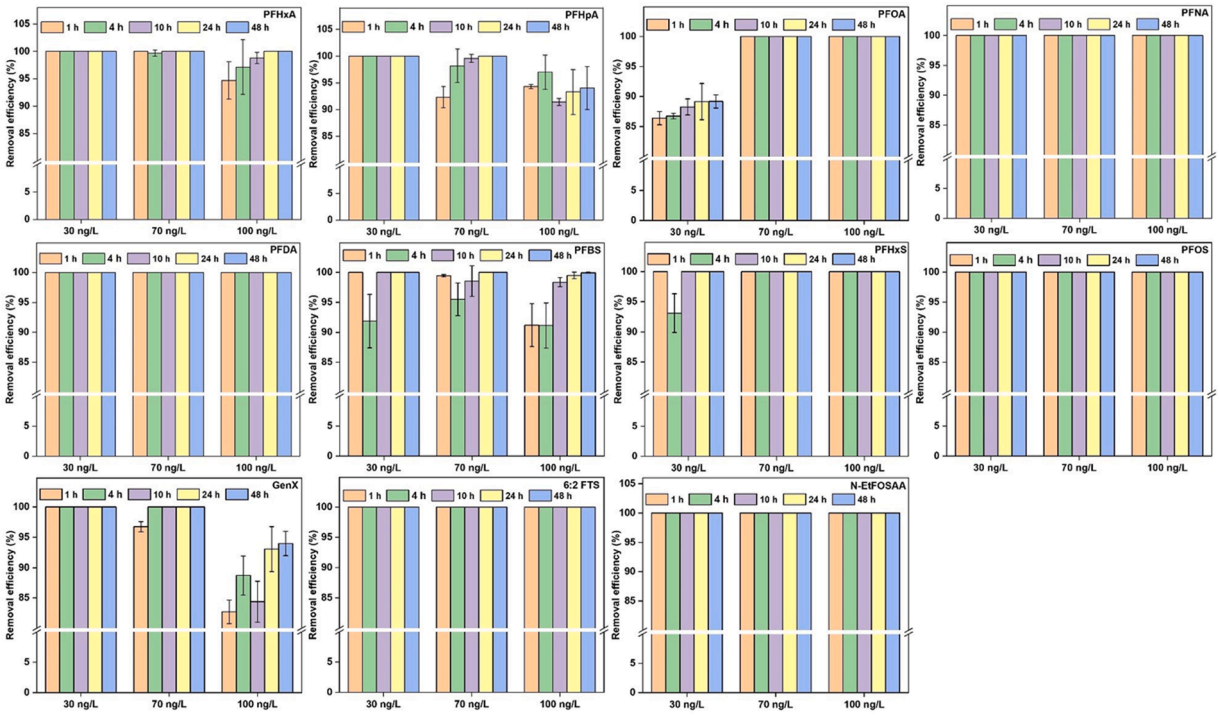

Fig. 3. Removal efficiency of PFAS spiked tap water. Initial PFAS concentration: 30, 70, or 100 ng/L, and flakes' dose: 500 mg/L. Error bars represent the standard deviations of triplicate measurements.

the negative impacts brought about by the anions and organic matter in tap water (Du et al., 2014; Kothawala et al., 2017). Regarding the tap water at the University at Albany, it is known to contain chloride at 24.8–30.2 mg/L, sulfate at 5.01–6.67 mg/L, and total organic carbon (TOC) at 1.41–2.06 mg/L in addition to other ions and chemicals (Kathy et al., 2022). The anions and TOC at mg/L concentrations that are at least 10,000 times higher than those of the PFAS, and may potentially interfere and compete with PFAS (Del Moral et al., 2020; Dixit et al., 2019; Maimaiti et al., 2018; Min et al., 2022) for adsorption sites on the flakes' surface.

Compared to other sorbents, the flakes' performance toward PFAS removal is much better. For example, magnetic ion exchange (MIEX)

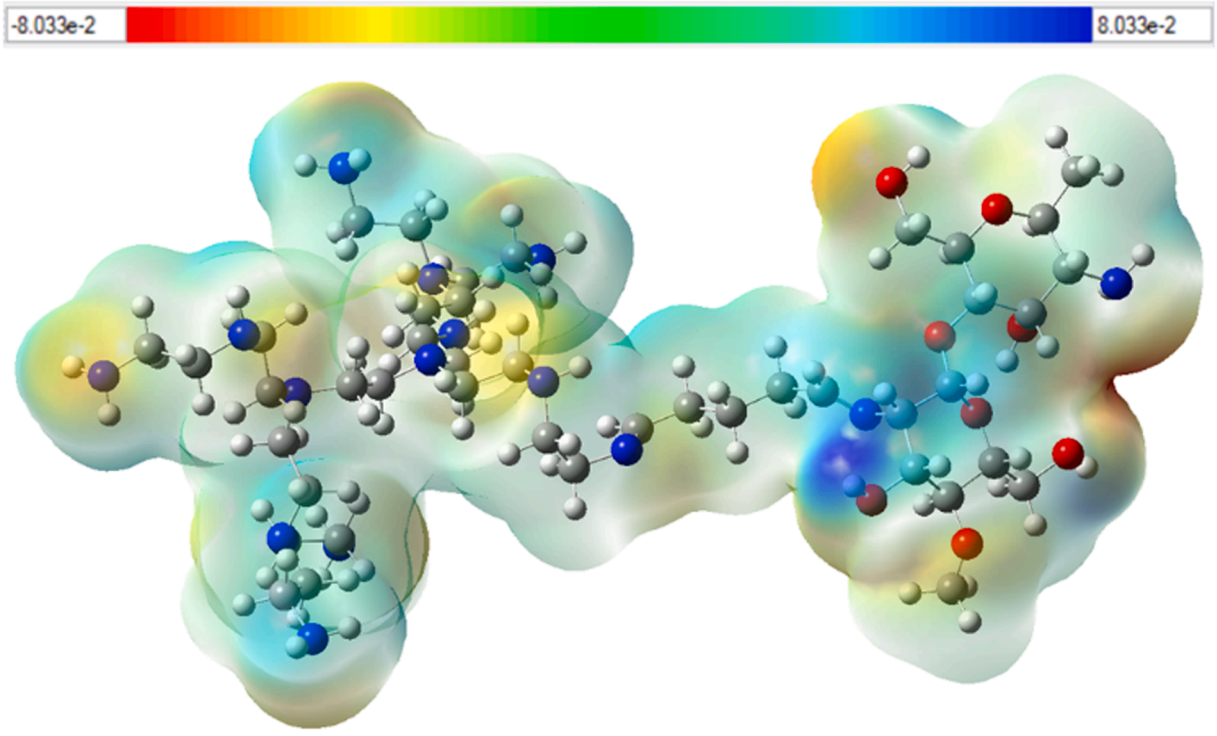

Fig. 4. The GTH—CTNPEI aerogel's molecular electrostatic potential surface, displaying regions of higher positive charge in blue and lower positive charge in red.

(Park et al., 2020) was reported to remove short chain PFCAs (C_4 and C_5), long chain PFCAs (C_6, and C_8), PFBS at 40–60 %, and PFOS and its isomers >90 % at 2 h in groundwater containing 10 % NaCl. A cationic polymer-based hydrogel (Ateia et al., 2019) was able to remove 75–95 % of PFSAs (C_4—C_8), and 60–80 % of PFCAs (C_4—C_8) and GenX, each at <1000 ng/L, from surface waters and treated wastewater at 24 h.

3.5. Mechanistic investigations of PFAS adsorption on GTH—CTNPEI at the molecular level

Using DFT simulations, we were able to identify the optimal adsorption sites and binding strength of GTH—CTNPEI aerogel with PFAS compounds at a molecular level (Yan et al., 2020). Using a M06–2X/6–31+*G*(d,p) basis set (Patel et al., 2022), the molecular electrostatic potential (MEP) map of GTH—CTNPEI aerogel was calculated, as illustrated in Fig. 4.

The different colors seen in the plots indicate distinct MEP surface values. The aerogel exhibits areas of low electron density (i.e., electrophilic regions). These are represented by the shades of light and dark blue, and are a consequence of the presence of the positively charged protonated amine groups of CTN and PEI. Consequently, they can be readily engaged by PFAS through electrostatic interactions, specifically COO^- and SO_3^- groups. The deepest red shade in the aerogel represents electron-rich regions where PFAS was not adsorbed due to electrostatic repulsion, while the green shade represents neutral regions of the MEP surface where hydrophobic interactions are expected to occur.

Figs. 5, S3 and S4 illustrate the positioning of three respective anionic PFAS (PFOA, PFOS, and PFBS) on the hydrophobic and electrostatic surface of the GTH—CTNPEI aerogel to evaluate the adsorption strength, (Ateia et al., 2019) which is represented by the binding energy (ΔE). As shown in Figs. 5B, S3 B, and S4 B, when located on the PEI side of the aerogel, PFOA, hydrophobic PFOS, and short-chain PFBS displayed higher ΔE values of −30.1, −48.5, and −47.3 kcal/mol, respectively, compared to the CTN and GTH cross-linkers side. Furthermore, both PFOS (Fig. S3) and PFBS (Fig. S4) had almost equal ΔE values that are higher than that of PFOA (Fig. 5). It was concluded that sulphonate PFAS strongly adsorbs to our aerogel compared to carboxylate PFAS due to its more hydrophobic nature.

By examining the interactions between PFAS and the GTH—CTNPEI aerogel, we were able to determine the values of Gibbs free energy (ΔG), which are displayed in Table S5. The values in Table S5 show that both long and short-chain PFAS had highly negative ΔG values ranging from −12 to −30 kcal/mol at different binding locations. In particular, the higher negative ΔG values are in alignment with what would be expected for PFAS adsorption when interacting with the PEI side of the aerogel (complex-II). Next, Tables S6, S7, and S8 show that the bond lengths of the C—F, C—O, and S—O of PFOA, PFOS, and PFBS respectively were shortened/enlarged after interacting with the GTH—CTNPEI aerogel due to hydrophobic and electrostatic interactions.

4. Conclusions

Computational modeling using DFT reveals that the surface of CTNPEI aerogels exhibits strong bonding interactions with both long-chain PFOA/PFOS and short-chain PFBS via hydrophobic and electrostatic forces. The fact that the GTH—CTNPEI aerogel flakes possess exceptionally high sorption capacity, are easily regenerated and reused, and result in >99 % removal of all tested PFAS at environmentally relevant concentrations in tap water, makes it a promising material for the removal of PFAS in other water matrices, such as surface water and groundwater. Compared with other sorption materials, its bio-based nature bestows better environmental sustainability in industrial scale production.

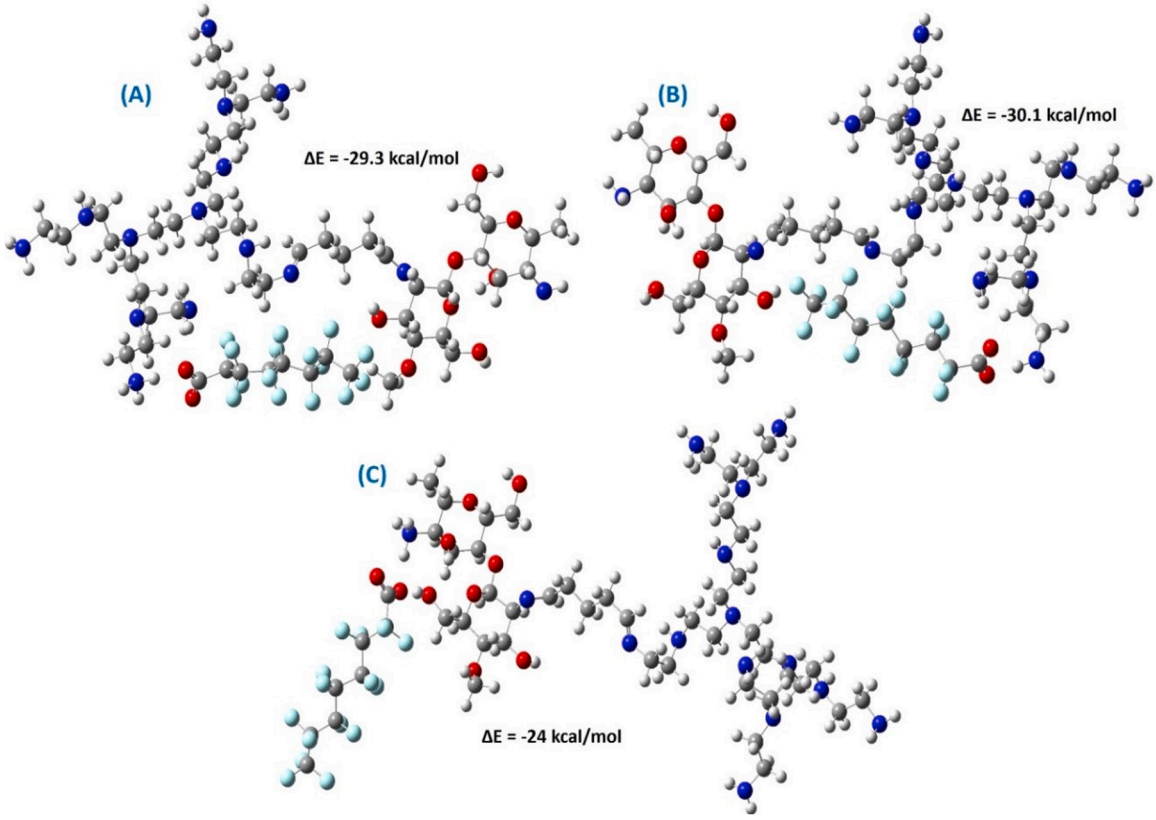

Fig. 5. Adsorption locations of: (A) PFOA/GTH—CTNPEI-I, (B) PFOA/GTH—CTNPEI-II and (C) PFOA/GTH—CTNPEI-III. The black, white, blue, cyan-blue, and red colors represent C, H, N, F and O-atoms, respectively.

Supporting information

The SI includes physiochemical properties of PFAS, PFAS analysis, PFAS adsorption capacity validation, PFAS adsorption in tap water, PFAS recovery results, and M06–2X/6–31+*G*(d,p) level optimized geometries and bond length measurements of PFAS, GTH—CTNPEI aerogel and various possible aerogel-PFAS complexes.

CRediT authorship contribution statement

Aswin Kumar Ilango: Conceptualization, Data curation, Formal analysis, Investigation, Methodology, Resources, Software, Validation, Visualization, Writing – original draft, Writing – review & editing. **Parandaman Arathala:** Conceptualization, Data curation, Formal analysis, Investigation, Methodology, Resources, Software, Validation, Visualization, Writing – review & editing. **Rabi A. Musah:** Conceptualization, Software, Writing – review & editing, Supervision. **Yanna Liang:** Funding acquisition, Project administration, Supervision, Validation, Visualization, Writing – review & editing, Methodology, Resources, Conceptualization.

Declaration of competing interest

The authors declare that they have no known competing financial interests or personal relationships that could have appeared to influence the work reported in this paper.

Data availability

Data will be made available on request.

Acknowledgment

The authors acknowledge financial support from the U.S. National Science Foundation under award number CBET 2225596. The authors are also thankful for the support of the High-Performance Computing Center at the University at Albany-SUNY.

Supplementary materials

Supplementary material associated with this article can be found, in the online version, at doi:10.1016/j.watres.2024.121458.

References

Arathala, P., Musah, R.A., 2020. Computational study investigating the atmospheric oxidation mechanism and kinetics of dipropyl thiosulfinate initiated by OH radicals and the fate of propanethiyl radical. J. Phys. Chem. A 124 (40), 8292–8304.
Arathala, P., Musah, R.A., 2022. Theoretical study of the atmospheric chemistry of methane sulfonamide initiated by OH radicals and the CH3S (O) 2N• H+ 3O2 reaction. J. Phys. Chem. A 126 (50), 9447–9460.
Ateia, M., Arifuzzaman, M., Pellizzeri, S., Attia, M.F., Tharayil, N., Anker, J.N., Karanfil, T., 2019. Cationic polymer for selective removal of GenX and short-chain PFAS from surface waters and wastewaters at ng/L levels. Water Res. 163, 114874.
Ateia, M., Attia, M.F., Maroli, A., Tharayil, N., Alexis, F., Whitehead, D.C., Karanfil, T., 2018. Rapid removal of poly-and perfluorinated alkyl substances by poly (ethylenimine)-functionalized cellulose microcrystals at environmentally relevant conditions. Environ. Sci. Technol. Lett. 5 (12), 764–769.
Bao, Y., Deng, S., Jiang, X., Qu, Y., He, Y., Liu, L., Chai, Q., Mumtaz, M., Huang, J., Cagnetta, G., 2018. Degradation of PFOA substitute: GenX (HFPO–DA ammonium salt): oxidation with UV/persulfate or reduction with UV/sulfite? Environ. Sci. Technol. 52 (20), 11728–11734.
Brendel, S., Fetter, É., Staude, C., Vierke, L., Biegel-Engler, A., 2018. Short-chain perfluoroalkyl acids: environmental concerns and a regulatory strategy under REACH. Environ. Sci. Eur. 30 (1), 9.
Brunn, H., Arnold, G., Körner, W., Rippen, G., Steinhäuser, K.G., Valentin, I., 2023. PFAS: forever chemicals—Persistent, bioaccumulative and mobile. Reviewing the status and the need for their phase out and remediation of contaminated sites. Environ. Sci. Eur. 35 (1), 1–50.
Buck, R.C., Franklin, J., Berger, U., Conder, J.M., Cousins, I.T., De Voogt, P., Jensen, A. A., Kannan, K., Mabury, S.A., van Leeuwen, S.P., 2011. Perfluoroalkyl and polyfluoroalkyl substances in the environment: terminology, classification, and origins. Integr. Environ. Assess. Manage 7 (4), 513–541.
Butenhoff, J.L., Chang, S.C., Ehresman, D.J., York, R.G., 2009. Evaluation of potential reproductive and developmental toxicity of potassium perfluorohexanesulfonate in Sprague Dawley rats. Reproduct. Toxicol. 27 (3–4), 331–341.
Ching, C., Lin, Z.W., Dichtel, W.R., Helbling, D.E., 2023. Evaluating the performance of novel cyclodextrin polymer granules to remove perfluoroalkyl acids (PFAAs) from water. ACS. EST Eng. 3 (5), 661–670.
Cordner, A., Goldenman, G., Birnbaum, L.S., Brown, P., Miller, M.F., Mueller, R., Patton, S., Salvatore, D.H., Trasande, L., 2021. The true cost of PFAS and the benefits of acting now. Environ. Sci. Technol. 55 (14), 9630–9633.
Del Moral, L.L., Choi, Y.J., Boyer, T.H., 2020. Comparative removal of Suwannee River natural organic matter and perfluoroalkyl acids by anion exchange: impact of polymer composition and mobile counterion. Water Res. 178, 115846.
Dixit, F., Barbeau, B., Mostafavi, S.G., Mohseni, M., 2019. PFOA and PFOS removal by ion exchange for water reuse and drinking applications: role of organic matter characteristics. Environ. Sci. Water Res. Technol. 5 (10), 1782–1795.
Dong, Q., Min, X., Huo, J., Wang, Y., 2021. Efficient sorption of perfluoroalkyl acids by ionic liquid-modified natural clay. Chem. Eng. J. Adv. 7, 100135.
Du, Z., Deng, S., Bei, Y., Huang, Q., Wang, B., Huang, J., Yu, G., 2014. Adsorption behavior and mechanism of perfluorinated compounds on various adsorbents—A review. J. Hazard. Mater. 274, 443–454.
EPA, U.S. (2021) U.S. EPA. Multi-Industry Per- and Polyfluoroalkyl Substances (PFAS) study –2021 preliminary report. U.S Environmental Protection Agency, Washington, DC. (2021).
Frisch, M.J., Trucks, G.W., Schlegel, H.B., Scuseria, G.E., Robb, M.A., Cheeseman, J.R., Scalmani, G., Barone, V., Petersson, G.A., Nakatsuji, H. and al., e. (2016) Gaussian 16. B.01, r. (ed), Gaussian, Inc., Wallingford, CT.
Gibert, O., Lefèvre, B., Fernández, M., Bernat, X., Paraira, M., Calderer, M., Martínez-Lladó, X., 2013. Characterising biofilm development on granular activated carbon used for drinking water production. Water Res. 47 (3), 1101–1110.
Giroday, T., Montero-Campillo, M.M., Mora-Diez, N., 2014. Thermodynamic stability of PFOS: M06-2X and B3LYP comparison. Comput. Theor. Chem. 1046, 81–92.
Glüge, J., London, R., Cousins, I.T., DeWitt, J., Goldenman, G., Herzke, D., Lohmann, R., Miller, M., Ng, C.A., Patton, S., 2021. Information requirements under the essential-use concept: PFAS case studies. Environ. Sci. Technol. 56 (10), 6232–6242.
Ilango, A.K., Jiang, T., Zhang, W., Feldblyum, J.I., Efstathiadis, H., Liang, Y., 2023a. Surface-modified biopolymers for removing mixtures of per- and polyfluoroalkyl substances from water: screening and removal mechanisms. Environ. Pollut. 331, 121865.
Ilango, A.K., Jiang, T., Zhang, W., Pervez, M.N., Feldblyum, J.I., Efstathiadis, H., Liang, Y., 2023b. Enhanced adsorption of mixtures of per- and polyfluoroalkyl substances in water by chemically modified activated carbon. ACS. EST Water. 3 (11), 3708–3715.
Ilango, A.K., Liang, Y., 2023. Surface modifications of biopolymers for removal of per- and polyfluoroalkyl substances from water: current research and perspectives. Water Res. 249, 120927.
Jiang, T., Zhang, W., Ilango, A.K., Feldblyum, J.I., Wei, Z., Efstathiadis, H., Yigit, M.V., Liang, Y., 2022. Surfactant-modified clay for adsorption of mixtures of per-and polyfluoroalkyl substances (PFAS) in aqueous solutions. ACS Appl. Eng. Mater. 1 (1), 394–407.
Jiang, X., Wang, W., Yu, G., Deng, S., 2021. Contribution of nanobubbles for PFAS adsorption on graphene and OH-and NH2-functionalized graphene: comparing simulations with experimental results. Environ. Sci. Technol. 55 (19), 13254–13263.
Karoyo, A.H., Wilson, L.D., 2013. Tunable macromolecular-based materials for the adsorption of perfluorooctanoic and octanoic acid anions. J. Colloid. Interface Sci. 402, 196–203.
Kathy M.S.; Joseph E.C., J, P.E. (2022) Annual Drinking Water Quality Report For 2022, City of Albany, USA.
Kothawala, D.N., Köhler, S.J., Östlund, A., Wiberg, K., Ahrens, L., 2017. Influence of dissolved organic matter concentration and composition on the removal efficiency of perfluoroalkyl substances (PFASs) during drinking water treatment. Water Res. 121, 320–328.
Li, J., He, J., Niu, Z., Zhang, Y., 2020. Legacy per-and polyfluoroalkyl substances (PFASs) and alternatives (short-chain analogues, F-53B, GenX and FC-98) in residential soils of China: present implications of replacing legacy PFASs. Environ. Int. 135, 105419.
Li, J., Li, X., Da, Y., Yu, J., Long, B., Zhang, P., Bakker, C., McCarl, B.A., Yuan, J.S., Dai, S. Y., 2022a. Sustainable environmental remediation via biomimetic multifunctional lignocellulosic nano-framework. Nat. Commun. 13 (1), 4368.
Li, R., Alomari, S., Stanton, R., Wasson, M.C., Islamoglu, T., Farha, O.K., Holsen, T.M., Thagard, S.M., Trivedi, D.J., Wriedt, M., 2021. Efficient removal of per-and polyfluoroalkyl substances from water with zirconium-based metal–organic frameworks. Chem. Mater. 33 (9), 3276–3285.
Li, X., Fatowe, M., Cui, D., Quinete, N., 2022b. Assessment of per-and polyfluoroalkyl substances in Biscayne Bay surface waters and tap waters from South Florida. Sci. Total Environ. 806, 150393.
Liu, W., Lin, T., Zhang, X., Jiang, F., Yan, X., Chen, H., 2022. Adsorption of perfluoroalkyl acids on granular activated carbon supported chitosan: role of nanobubbles. Chemosphere 309, 136733.
Maimaiti, A., Deng, S., Meng, P., Wang, W., Wang, B., Huang, J., Wang, Y., Yu, G., 2018. Competitive adsorption of perfluoroalkyl substances on anion exchange resins in simulated AFFF-impacted groundwater. Chem. Eng. J. 348, 494–502.
Marenich, A.V., Cramer, C.J., Truhlar, D.G., 2009. Universal solvation model based on solute electron density and on a continuum model of the solvent defined by the bulk dielectric constant and atomic surface tensions. J. Phys. Chem. B 113 (18), 6378–6396.

Márquez, P., Benítez, A., Chica, A.F., Martín, M.A., Caballero, A., 2022. Evaluating the thermal regeneration process of massively generated granular activated carbons for their reuse in wastewater treatments plants. J. Clean. Prod. 366, 132685.
McCleaf, P., Englund, S., Östlund, A., Lindegren, K., Wiberg, K., Ahrens, L., 2017. Removal efficiency of multiple poly-and perfluoroalkyl substances (PFASs) in drinking water using granular activated carbon (GAC) and anion exchange (AE) column tests. Water Res. 120, 77–87.
Militao, I.M., Roddick, F.A., Bergamasco, R., Fan, L., 2021. Removing PFAS from aquatic systems using natural and renewable material-based adsorbents: a review. J. Environ. Chem. Eng. 9 (4), 105271.
Min, X., Huo, J., Dong, Q., Xu, S., Wang, Y., 2022. Enhanced sorption of perfluorooctanoic acid with organically functionalized layered double hydroxide. Chem. Eng. J. 446, 137019.
Park, M., Daniels, K.D., Wu, S., Ziska, A.D., Snyder, S.A., 2020. Magnetic ion-exchange (MIEX) resin for perfluorinated alkylsubstance (PFAS) removal in groundwater: roles of atomic charges for adsorption. Water Res. 181, 115897.
Patel, S.G., Vala, R.M., Patel, P.J., Upadhyay, D.B., Ramkumar, V., Gardas, R.L., Patel, H. M., 2022. Synthesis, crystal structure and in silico studies of novel 2, 4-dimethoxy-tetrahydropyrimido [4, 5-b] quinolin-6 (7 H)-ones. RSC Adv. 12 (29), 18806–18820.
Peverati, R., Truhlar, D.G., 2014. Quest for a universal density functional: the accuracy of density functionals across a broad spectrum of databases in chemistry and physics. Philos. Trans. R. Soc. A 372 (2011), 20120476. Mathematical, Physical and Engineering Sciences.
Rabinow, L. (2022) Parts per Trillion.
Rayne, S., Forest, K., 2010. Theoretical studies on the pKa values of perfluoroalkyl carboxylic acids. J. Mol. Struct. Theochem. 949 (1), 60–69.
Ren, Z., Bergmann, U., Uwayezu, J.N., Carabante, I., Kumpiene, J., Lejon, T., Leiviskä, T., 2023. Combination of adsorption/desorption and photocatalytic reduction processes for PFOA removal from water by using an aminated biosorbent and a UV/sulfite system. Environ. Res. 228, 115930.
Saha, D., Khan, S., Van Bramer, S.E., 2021. Can porous carbons be a remedy for PFAS pollution in water? A perspective. J. Environ. Chem. Eng. 9 (6), 106665.
Smalling, K.L., Romanok, K.M., Bradley, P.M., Morriss, M.C., Gray, J.L., Kanagy, L.K., Gordon, S.E., Williams, B.M., Breitmeyer, S.E., Jones, D.K., 2023. Per-and polyfluoroalkyl substances (PFAS) in United States tapwater: comparison of underserved private-well and public-supply exposures and associated health implications. Environ. Int., 108033
Son, H., Kim, T., Yoom, H.S., Zhao, D., An, B., 2020. The adsorption selectivity of short and long per-and polyfluoroalkyl substances (PFASs) from surface water using powder-activated carbon. Water. (Basel) 12 (11), 3287.
Sunderland, E.M., Hu, X.C., Dassuncao, C., Tokranov, A.K., Wagner, C.C., Allen, J.G., 2019. A review of the pathways of human exposure to poly-and perfluoroalkyl substances (PFASs) and present understanding of health effects. J. Expo Sci. Environ. Epidemiol. 29 (2), 131–147.
Teymoorian, T., Munoz, G., Vo Duy, S., Liu, J., Sauvé, S., 2023. Tracking PFAS in drinking water: a review of analytical methods and worldwide occurrence trends in tap water and bottled water. ACS. EST Water 3 (2), 246–261.
Vu, C.T., Wu, T., 2020. Adsorption of short-chain perfluoroalkyl acids (PFAAs) from water/wastewater. Environ. Sci. Water Res. Technol. 6 (11), 2958–2972.
Vu, C.T., Wu, T., 2022. Recent progress in adsorptive removal of per-and poly-fluoroalkyl substances (PFAS) from water/wastewater. Crit. Rev. Environ. Sci. Technol. 52 (1), 90–129.
Wang, Z., Cousins, I.T., Scheringer, M., Hungerbuehler, K., 2015. Hazard assessment of fluorinated alternatives to long-chain perfluoroalkyl acids (PFAAs) and their precursors: status quo, ongoing challenges and possible solutions. Environ. Int. 75, 172–179.
Watanabe, N., Takata, M., Takemine, S., Yamamoto, K., 2018. Thermal mineralization behavior of PFOA, PFHxA, and PFOS during reactivation of granular activated carbon (GAC) in nitrogen atmosphere. Environ. Sci. Pollut. Res. 25, 7200–7205.
Woodard, S., Berry, J., Newman, B., 2017. Ion exchange resin for PFAS removal and pilot test comparison to GAC. Remed. J. 27 (3), 19–27.
Wu, C., Klemes, M.J., Trang, B., Dichtel, W.R., Helbling, D.E., 2020. Exploring the factors that influence the adsorption of anionic PFAS on conventional and emerging adsorbents in aquatic matrices. Water Res. 182, 115950.
Yan, B., Munoz, G., Sauvé, S., Liu, J., 2020. Molecular mechanisms of per-and polyfluoroalkyl substances on a modified clay: a combined experimental and molecular simulation study. Water Res. 184, 116166.
Zaggia, A., Conte, L., Falletti, L., Fant, M., Chiorboli, A., 2016. Use of strong anion exchange resins for the removal of perfluoroalkylated substances from contaminated drinking water in batch and continuous pilot plants. Water Res. 91, 137–146.
Zhao, Y., Truhlar, D.G., 2006. A density functional that accounts for medium-range correlation energies in organic chemistry. Org. Lett. 8 (25), 5753–5755.
Zhao, Y., Truhlar, D.G., 2008. The M06 suite of density functionals for main group thermochemistry, thermochemical kinetics, noncovalent interactions, excited states, and transition elements: two new functionals and systematic testing of four M06-class functionals and 12 other functionals. Theor. Chem. Acc. 120, 215–241.